Microsc. Microanal. Microstruct. **1** (1990) 167–173 JUNE **1990**, PAGE 167

Classification
Physics Abstracts
61.14D — 61.16D

Two remarkable defect related electron diffraction effects

Marc Verwerft(*), Wout Luyten and Severin Amelinckx

University of Antwerp (R.U.C.A.) Groenenborgerlaan, 171 B-2020 Antwerp, Belgium

(Received June 28, 1990; accepted July 11, 1990)

Résumé. — Dans cette note, nous présentons et interprétons deux effets remarquables de diffraction électronique. Dans les deux cas, leur interprétation n'est possible qu'en l'associant à une information obtenue dans l'expace réel sur les défauts présents localement dans l'échantillon. Une première observation est un cas particulier de phénomène de "double" diffraction mettant en jeu deux portions cristallines de stuctures différentes. La seconde réside dans un effet interférentiel apparaissant dans des structures d'intercroissance.

Abstract. — In this note, two singular diffraction effects are reported and interpreted. For the two cases presented here, the interpretation of the diffraction pattern is only possible when combined with real space information about the defects in the material. A first observation is that of a peculiar case of so called "double" diffraction involving two crystal parts with a different structure. The second observation is that of an interference effect occuring at intergrowth structures.

1. Introduction.

Although most interference effects due to electrons have been widely studied and the diffraction of electrons by solids is quite well understood, some unexpected aspects of known diffraction effects may still cause puzzling patterns and possibly give rise to interpretation difficulties. In this paper we shall discuss two such effects which arose in the electron diffraction associated with second phases in crystals. In both cases the interpretation of the diffraction patterns would have been difficult without a knowledge of direct space as deduced from imaging and sometimes might lead to erroneous conclusions. The correct interpretation on the other hand allows to derive some additional information of interest.

2. Voidite in diamond.

2.1 OBSERVATIONS. — A remarkable diffraction pattern was observed when studying diamond crystals containing voids : so called "voidite" [1, 2]. Some examples of diffraction patterns are

(*) Research assistant of the National Fund for Scientific Research (Belgium)

shown in figures 1a and b as taken along a cube direction [001] of diamond. Apart from the strong diamond spots and the corresponding Kikuchi lines and bands one notes sometimes weak spots forming an array of spots identical with the zone axis pattern, but shifted over a vector **R**. The weak spots are only produced when a void is present in the selected area, such a void is shown in figure 2. It is thus clear that the presence of the weak spots is related to that of the void. However the array of weak spots does not reveal the diffraction pattern of this precipitate or inclusion called void, but it has the characteristics of the diamond reciprocal lattice. A schematic representation of the observed diffraction pattern is shown in the inset of figure 3. The vector **R** is different for the different diffraction patterns. When plotting the $\mathbf{R}_i$ vectors observed along a given zone of the diamond lattice, the endpoints of the $\mathbf{R}_i$ form a lattice, different from the diamond lattice, but representative for the precipitate structure as we shall show.

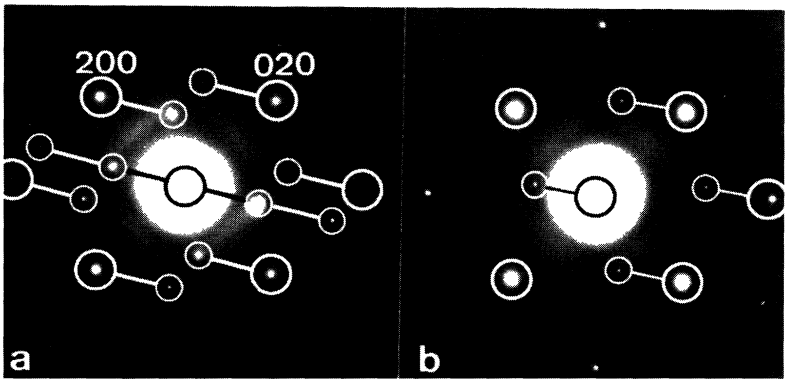

Fig. 1. — (a) and (b) Different diffraction patterns along the cube zone of diamond observed in an area containing a void.

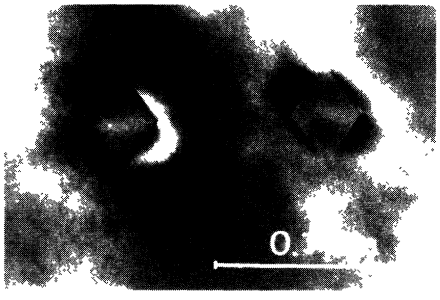

Fig. 2. — Voids in diamond imaged at high resolution. Note the octahedral shape of the voids.

2.2 DISCUSSION. — We shall show that the observed weak spots are due to diffraction by diamond, the incident beam being produced by the precipitate. The reciprocal space construction is represented in figure 3. The primary incident beam **1** and the corresponding Ewald sphere (represented by a plane) is E_1 ; it intersects the spikes of the reciprocal lattice of diamond in the points

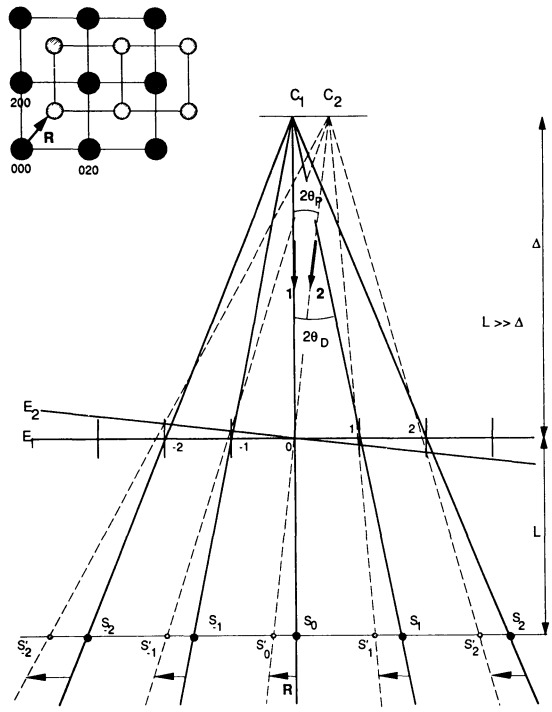

Fig. 3. — Schematic representation of the diffraction pattern produced when a void is present in the selected area. Inset : reciprocal lattice construction illustrating how a weak diamond diffraction pattern is formed in the presence of a void.

-2, -1, 0, 1, 2 producing the spots S_{-2}, S_{-1}, S_0, S_1, S_2 on the plate. Let us assume now that when the incident beam hits the precipitate, one (or a small number of) strong Bragg reflection(s) is produced, the diffracted beam enclosing an angle of $2\Theta_p$ with the primary incident beam (p : precipitate). The small size of the precipitate makes it easier to excite strong reflections since the Bragg condition is relaxed along all directions of the precipitate. This secondary incident beam has now the direction **2**. Due to the epitaxial orientation relationship between inclusion and diamond, the Bragg angle Θ_p will not be very different from a possible Bragg angle of diamond. The "secondary" incident beam will thus be close to a Bragg orientation for the subsequent diamond crystal part. Moreover since the diamond specimen as a whole has the shape of a thin foil, several Bragg reflections can be simultaneously excited in the diamond. The part of the diamond behind the precipitate produces a diffraction pattern with this beam **2** as the incident beam i.e. the centre of Ewald's sphere becomes C_2 and Ewald's sphere is now E_2.

Constructing the diffracted beams leads to the diffraction pattern..., S'_1, S'_0, S'_1,... Since the Bragg angles are very small, the spot shifts are to a good approximation all the same i.e.

$$\mathbf{R} = S_0S'_0 = S_{-1}S'_{-1} = S_1S'_1 = \ldots$$

with $\mathbf{R} = 2L\Theta_p$ where L is the distance between the specimen and the plate (i.e. the camera length). The measurement of the $\mathbf{R}_i$ thus allows to determine the Bragg angles Θ_p of the precipitate and thus allows its identification.

If the precipitate produces more than one strong beam, several zone arrays of weak diamond diffraction spots will be produced, one with each secondary incident beam as origin (Fig. 1a). The number of such secondary incident beams is small since only the most strongly excited reflections of the precipitate will give rise to a diamond diffraction pattern. Also the secondary incident beam will be relatively weak since its intensity is related to the size of the precipitate.

The phenomenon described, can be considered as a peculiar form of "double" diffraction, the two crystal parts involved having a different structure however. It is also related to the diffraction phenomena leading to Moiré patterns. From a number of different diffraction patterns of the type described, the diffraction pattern of the matter present in the voids could be derived. These results will be published elsewhere.

3. Double slit diffraction in $Nd_{1-x}Ce_xCuO_4$.

3.1 OBSERVATIONS. — Recently, electron superconductivity has been discovered in the materials $Ln_{1-x}Ce_xCuO_4$(Ln = Pr, Nd, Sm) [3]. In the course of an electron microscopy study of the superconductor $Nd_{1-x}Ce_xCuO_4$, we noted that often coherently intergrown very thin lamellae of a second phase were present. Figure 4a shows an area containing several such lamellae ; most of these occur isolated, but occasionally they occur in close pairs, as shown in the inset. The high resolution image of one lamella is shown in figure 4b ; it proves that the "slits" consist of a different material from that of the bulk. The composition of the intergrown lamellae is most probably Nd_2O_3, but this is not important for the phenomenon to be described here.

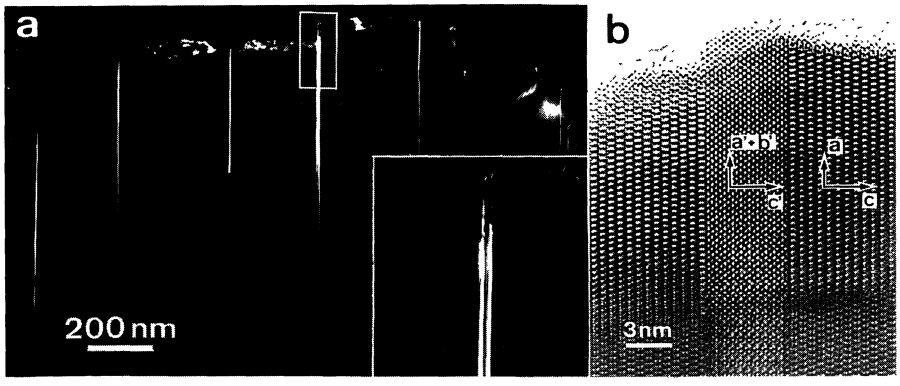

Fig. 4. — (a) Dark field image in an intergrowth reflection of a foil of $Nd_{1-x}Ce_xCuO_4$ containing thin lamellae of an intergrown structure. Inset : higher magnification of two closely spaced lamellae. (b) High resolution image of one lamella.

The diffraction pattern of an area containing a single lamella is shown in the inset of figure 5 ; the weak spots which are due to the material within the lamella are very much broadened due to its small thickness. The intensity distribution is that described by the well known slit function $\frac{\sin^2(2\pi ah)}{(2\pi ah)^2}$ where $2a$ is the slitwidth. The diffraction pattern of a selected area containing a close pair of such lamellae is shown in figure 5. The zone axis with respect to the $Nd_{1-x}Ce_xCuO_4$ host crystal is [010]. The host crystal produces the pattern of intense spots. However sequences of

closely spaced weak additional spots are present, which would suggest the presence of a compound with a very long spacing of $\approx$ 7.5 nm. However we shall show that this is not the case. The weak spots are due to the presence of the thin lamellae since they are absent when the selected area does not contain a pair of thin lamellae of the second phase.

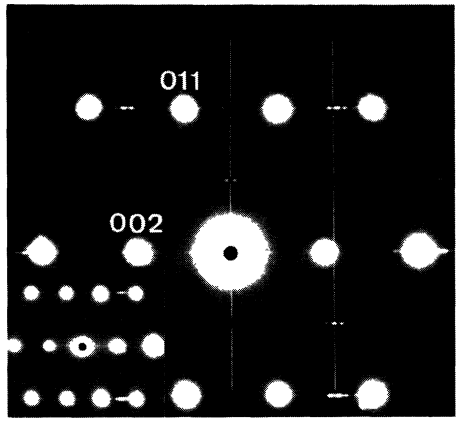

Fig. 5. — Diffraction pattern resulting from two intergrowths and the $Nd_{1-x}Ce_xCuO_4$ matrix. The arrays of spots result from interference between electrons scattered by two closely spaced lamellae. Inset : Diffraction pattern resulting from one intergrowth and the $Nd_{1-x}Ce_xCuO_4$ matrix : spots corresponding with the intergrowth are streaked due to the small c'-dimension.

3.2 MODEL. — As a model for the description of the diffraction effect due to the double slit, we assume that both slits are infinitely long along the y-direction and a width $2a$ along the x-direction ; the central lines of the slits are separated by a distance $2D$ (inset of Fig. 6). Only the material within the slits is assumed to be diffracting, the diffraction effect being described by the lattice potential $V(\mathbf{r})$. The lattice potentials within the two slits are the same except for a possible shift. Let

$$V_1(\mathbf{r}) = \sum_{\mathbf{g}} V_{\mathbf{g}} \exp(2\pi i\, \mathbf{g} \cdot \mathbf{r}) \tag{1}$$

be the lattice potential in the first slit. Let us assume that the structure which is the same within the second slit is shifted over $\mathbf{R}$ with respect to that present in the first slit. We then have :

$$\begin{aligned} V_2(\mathbf{r}) &= \sum_{\mathbf{g}} V_{\mathbf{g}} \exp(2\pi i\, \mathbf{g} \cdot (\mathbf{r} + \mathbf{R})) \\ &= \sum_{\mathbf{g}} (V_{\mathbf{g}} \exp(2\pi i\, \mathbf{g} \cdot \mathbf{R}))\, \exp(2\pi i\, \mathbf{g} \cdot \mathbf{r}) \end{aligned} \tag{2}$$

i.e. the fourier coefficient $V_{\mathbf{g}}$ has acquired a phase factor $\exp(2\pi i\, \mathbf{g} \cdot \mathbf{R})$. The lattice potential is assumed to be zero outside the slits. We can then introduce slit functions $\phi_j(\mathbf{r})$ which essentially

depend on x only and are defined as :

$$\Phi_1(\mathbf{r}) = 1 \text{ for } -D-a < x < -D+a$$
$$= 0 \text{ elsewhere.}$$

$$\Phi_2(\mathbf{r}) = 1 \text{ for } D-a < x < D+a$$
$$= 0 \text{ elsewhere.}$$

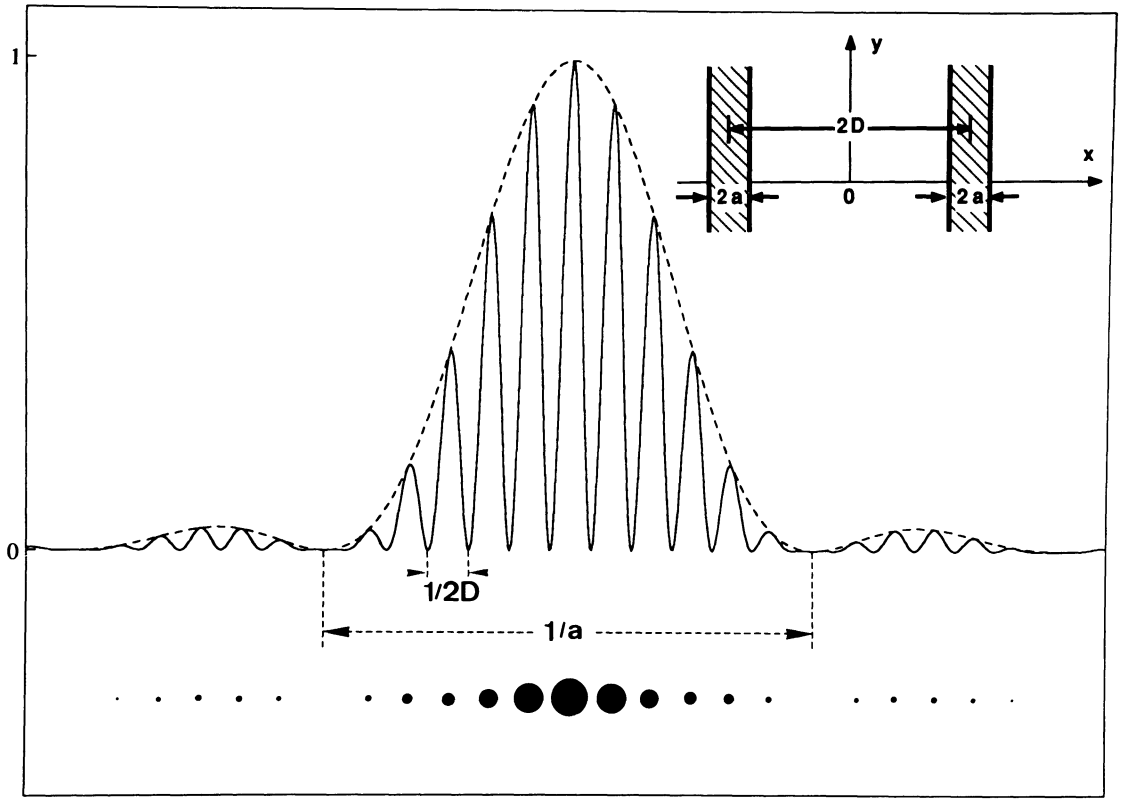

Fig. 6. — Schematic representation of the intensity distribution in the clusters of spots due to the interference between the beams diffracted by the thin lamellae for the case $\alpha_g = 0$. Inset : schematic representation of the double slit function.

The direct space configuration that produces the diffraction pattern of interest can by represented by $V_1(\mathbf{r})\Phi_1(\mathbf{r}) + V_2(\mathbf{r})\Phi_2(\mathbf{r})$.

3.3 DISCUSSION. — The fourier transform of the double slit can then be written as :

$$A(\mathbf{h}) = \int_{\mathbf{R}^3} [V_1(\mathbf{r})\Phi_1(\mathbf{r}) + V_2(\mathbf{r})\Phi_2(\mathbf{r})] \, (\exp(-2\pi i \, \mathbf{h} \cdot \mathbf{r})) \, d\mathbf{r} \qquad (3)$$

The integration along the y and z directions extends from $-\infty$ to $+\infty$ while the integration along x is limited to the two intervals mentioned above. Calling g_x, g_y, g_z and h_x, h_y, h_z the components of $\mathbf{g}$ and $\mathbf{h}$ along the directions x, y and z respectively, the amplitude $A(\mathbf{h})$ can be written as :

$$A(\mathbf{h}) = \sum_{\mathbf{g}} V_{\mathbf{g}}\, \delta(g_y - h_y)\, \delta(g_z - h_z) \left[\frac{\sin 2\pi (g_x - h_x)\, a}{\pi (h_x - g_x)}\right] \{\exp(-2\pi i (g_x - h_x)\, D) + \\ + \exp(2\pi i (g_x - h_x)\, D) \exp(2\pi i\, \mathbf{g} \cdot \mathbf{R})\} \tag{4}$$

The function between square brackets is peaked at $h_x = gx$ i.e. at the node positions of the reciprocal lattice of the structure present within the slits i.e. at $\mathbf{h} = \mathbf{g}$. After introducing $\alpha_{\mathbf{g}} = \mathbf{g} \cdot \mathbf{R}$, we can formulate the result as :

$$A(\mathbf{h}) = 4a \sum_{\mathbf{g}} V_{\mathbf{g}} \exp(\pi i \alpha_{\mathbf{g}})\, \delta(g_y - h_y)\, \delta(g_z - h_z) \left[\frac{\sin 2\pi (g_x - h_x)\, a}{2\pi (h_x - g_x)\, a}\right] \times \\ \times \cos 2\pi ((g_x - h_x)\, D - \alpha_{\mathbf{g}}/2) \tag{5}$$

The diffracted intensity is given by the square of the amplitude. At the nodes ($\mathbf{g}$) of the reciprocal lattice of the structure of the lamellae, a series of reflections (represented schematically in Fig. 6) separated by $1/2D$ and attenuated by the slit function envelope is observed. In the particular case of interest for our observations (Fig. 5), the positions of the reciprocal lattice node are in the middle between two weak spots if $h+k$ is odd, whereas it coincides with a spot if $h+k$ = even. This corresponds with $\mathbf{R} = 1/2[110]$; we then have $\alpha_{\mathbf{g}} = 1/2(h + k)$ and the sequence of diffraction spots of which the positions are essentially given by the extrema of $\cos 2\pi (h_{\mathbf{g}} D - \alpha/2)$ will be shifted with respect to the nodes of the reciprocal lattice over $\frac{1}{4D}$ if $h + k$ is odd.

The separation of the weak spots in figure 5 is found to be consistent within the experimental error with the observed separation of the slits in figure 4a.

4. Conclusions.

Two remarkable electron diffraction effects, both related to the presence of a second phase are described and the underlying kinematical theory necessary for their interpretation has been presented. These phenomena illustrate the need to combine information from direct and reciprocal space in order to be able to interpret diffraction patterns correctly.

Acknowledgements.

We thank Dr. G. S. Woods (C.S.O. Valuation, A. G.) for providing diamond containing voidite ; Dr. W. Sadowski (Geneva University) for providing samples of $Nd_{1-x}Ce_xCuO_4$ and Prof. Dr. G. Van Tendeloo and Prof. Dr. J. Van Landuyt for useful discussions.

References

[1] HIRSCH P. B., HUTCHISON J. L., TITCHMARSH J. M., *Philos. Mag. A* **54** (1986) L49.
[2] VAN TENDELOO G., LUYTEN W., WOODS G. S., *Philos. Mag. lett.* **61** (1990) 343.
[3] TOKURA Y., TAKAGI H., UCHIDA S., *Nature* **337** (1989) 345.

Cet article a été imprimé avec le Macro Package "Editions de Physique Avril 1990".